HHS Public Access

Author manuscript

*Mol Cell*. Author manuscript; available in PMC 2016 August 06.

Published in final edited form as:

*Mol Cell*. 2015 August 6; 59(3): 502–511. doi:10.1016/j.molcel.2015.06.022.

# An interactive database for the assessment of histone antibody specificity

**Scott B. Rothbart**[1,*], **Bradley M. Dickson**[1], **Jesse R. Raab**[2,3], **Adrian T. Grzybowski**[4], **Krzysztof Krajewski**[5], **Angela H. Guo**[5], **Erin K. Shanle**[5], **Steven Z. Josefowicz**[6], **Stephen M. Fuchs**[7], **C. David Allis**[6], **Terry R. Magnuson**[2,3], **Alexander J. Ruthenburg**[4,8], and **Brian D. Strahl**[3,5,*]

[1]Center for Epigenetics, Van Andel Research Institute, Grand Rapids, Michigan 49503, USA

[2]Department of Genetics, University of North Carolina at Chapel Hill, Chapel Hill, North Carolina 27599, USA

[3]Lineberger Comprehensive Cancer Center, University of North Carolina at Chapel Hill, Chapel Hill, North Carolina 27599, USA

[4]Department of Molecular Genetics and Cell Biology, The University of Chicago, Chicago, Illinois 60637, USA

[5]Department of Biochemistry and Biophysics, University of North Carolina at Chapel Hill, Chapel Hill, North Carolina 27599, USA

[6]Laboratory of Chromatin Biology and Epigenetics, The Rockefeller University, New York, New York 10065, USA

[7]Department of Biology, Tufts University, Medford, Massachusetts 02155, USA

[8]Department of Biochemistry and Molecular Biology, The University of Chicago, Chicago, Illinois 60637, USA

## SUMMARY

Access to high quality antibodies is a necessity for the study of histones and their posttranslational modifications (PTMs). Here we debut The Histone Antibody Specificity Database (http://www.histoneantibodies.com), an online and expanding resource cataloguing the behavior of widely used commercially available histone antibodies by peptide microarray. This interactive web portal provides a critical resource to the biological research community who routinely use these antibodies as detection reagents for a wide range of applications.

[*]Correspondence: (brian_strahl@med.unc.edu, 919-843-3896; scott.rothbart@vai.org, 616-234-5367).

## INTRODUCTION

Histones and their numerous posttranslational modifications (PTMs) are fundamental to the process of cell fate decision-making and organismal development. Consistent with this, studies have shown that both histone mutation and PTM misregulation contribute to the initiation and progression of a wide number of human diseases, including cancer and neurological disorders (Bannister and Kouzarides, 2011; Dawson and Kouzarides, 2012; Funato et al., 2014; Jakovcevski and Akbarian, 2012; Lewis et al., 2013; Rothbart and Strahl, 2014). Histone modifications function in part as docking sites for effector proteins harboring specialized, evolutionarily conserved domains that 'read' the single or combinatorial modification states of histones (Gardner et al., 2011; Jenuwein and Allis, 2001; Strahl and Allis, 2000).

The mass production and distribution of PTM-specific histone antibodies (more than 1,000 are commercially available to date) has greatly facilitated the study of these histone marks and their impact on chromatin function (Perez-Burgos et al., 2004; Turner and Fellows, 1989). Histone PTM antibodies are essential for numerous applications in chromatin research, including immunoblotting, immunostaining, and chromatin immunoprecipitation (ChIP). Indeed, large-scale epigenomics 'roadmap' efforts like the Encyclopedia of DNA Elements (ENCODE) projects depend on these antibodies for genome-wide mapping of histone PTM distribution (Ernst et al., 2011; Gerstein et al., 2010; Kharchenko et al., 2011). However, recent studies have made some surprising and alarming observations regarding the behavior of histone PTM antibodies, including off-target recognition, strong influence by neighboring PTMs, and an inability to distinguish the modification state on a particular residue (e.g., mono-, di-, or tri-methyl lysine) (Bock et al., 2011; Egelhofer et al., 2011; Fuchs et al., 2011; Fuchs and Strahl, 2011; Hattori et al., 2013; Nishikori et al., 2012; Rothbart et al., 2012e). Consequently, poor antibody choice can lead to misinformed conclusions regarding the location and function of the histone PTM being queried (Baker, 2015). As our understanding of how histone PTMs contribute to normal biology and human disease depends on the quality of the antibodies being used, continued rigorous quality control is needed for accurate data interpretation and continued progress in the field.

Herein, we describe an interactive web resource, The Histone Antibody Specificity Database, for histone PTM antibody characterization built on our recently developed high-density histone peptide microarray platform (Fuchs et al., 2011; Rothbart et al., 2012b). This open-access database, which at the time of publication provides characterization data on over 100 of the most frequently used and cited commercially available histone PTM antibodies, serves as an interactive, sustained and evolving platform for the interrogation of antibody specificity that will greatly aid epigenetics researchers in making more informed histone antibody choices. We provide several vignettes of common antibody behavior drawn from this resource, including off-target recognition and sensitivity to neighboring PTMs, and we highlight how these behaviors could influence the conclusions made from their use in various applications.

# RESULTS

## The Histone Antibody Specificity Database

We recently developed a high-density histone peptide microarray platform consisting of a library of over 250 purified biotinylated histone peptides harboring PTMs (lysine acetylation, lysine/arginine methylation, and serine/threonine phosphorylation) alone and in relevant combinations that are largely derived from mass spectrometry-based proteomics datasets (Table S1**)** (Pesavento et al., 2008; Sidoli et al., 2012; Young et al., 2009; Young et al., 2010). This platform allows for robust and comprehensive characterization of the behavior of histone-interacting proteins, including the specificity of histone antibodies (Figure 1A) (Cai et al., 2013; Fuchs et al., 2011; Rothbart et al., 2013; Rothbart et al., 2012a; Rothbart et al., 2012e). Notably, antibody reactivity with differing modification states (e.g., mono-, di- and trimethyl lysine) and the influence of epitope recognition by neighboring histone PTMs can be determined with high precision. With this platform, we analyzed over 100 histone PTM antibodies that are commercially available from nine suppliers who market these products to specifically recognize various methylated, acetylated, and phosphorylated residues (and their combinations) on the core and variant histones, yielding over 25,000 specific binding measurements (Figure 1B and Table S2).

To create a versatile platform that is easily accessible to the broad scientific community for interrogation of histone antibody specificity data, we built an interactive web platform, www.histoneantibodies.com (Figure 1C), which utilizes the D3js JavaScript library. Users can query the database by search bar (Figure 1C; **top**) or by histone and sequence context (Figure 1C**; bottom**) for antibody data specified by PTM of interest, histone, residue, company, or product number (Table S2). All datasets for a particular PTM of interest are presented together to allow users to make direct comparisons. Data are presented on the website as interactive heat maps (Figures S1A and S1B) and bar graphs (Figure S1B). Hovering over individual data points in these graphs gives the user information on corresponding peptide length, PTMs, and sequence context (Table S1). For heat maps, array signal intensities are ordered from strongest (yellow) to weakest (blue) relative to a reference target (black) – the peptide harboring the PTM(s) on the antibody product label. All peptides containing the reference target are outlined in red.

For bar graphs, array results are presented as normalized mean intensities ± S.E.M. on a scale from 0 (undetectable binding) to 1 (strong binding). The target peptide is depicted as a green bar. Orange bars indicate target-containing peptides that display enhanced signal compared to the reference. These are PTM combinations that enhance antibody binding. Light blue bars indicate target-containing peptides that display a diminished signal compared to the reference. These are PTM combinations that inhibit antibody binding. Gray bars indicate off-target peptides. Analysis of all tested histone PTM antibodies allowed us to bin unfavorable behavior into three general categories: 1) an inability to distinguish states of methylated lysine, 2) sensitivity to neighboring PTMs, and 3) recognition of off-target modifications. Examples of these types of behavior are discussed below.

## Distinguishing States of Methylated Lysine

Of the 38 di- and tri-methyllsyine antibodies screened, 16 cross-react with lower states of lysine methylation on a target residue, and one recognized a higher state of lysine methylation. Notably, this does not appear to be a general property of methyllysine antibodies to a particular target residue. For example, analysis of five H3K4me3 antibodies shows that several cross-react with H3K4me2 peptides, while others are selective for the H3K4me3 mark (Figure 2A**, left**). This is also true for H3K4me2 antibodies, some of which cross-react with H3K4me1 peptides (Figure 2A**, right**). Importantly, the three states of methylation at H3K4 have reportedly differential regulatory functions (Barski et al., 2007), yet analysis of the genomic distribution of these marks by ChIP-Seq in HEPG2 cells, using antibodies that cross react with lower order methylation states by microarray, shows overlapping signal for H3K4me3 and H3K4me2 across transcription start sites and gene bodies (Figure S2A), and for H3K4me2 and H3K4me1 across enhancer elements (Figure S2B). Collectively, these results highlight the importance of antibody choice for accurately discerning between various states of lysine methylation and suggest antibody cross-reactivity may contribute to inaccurate mapping of histone lysine methylation states in genome-wide analyses due to antibody cross-reactivity.

## Sensitivity to neighboring PTMs

Neighboring PTMs can impact not only the ability of a reader domain to bind its target modification but also the ability of histone PTM antibodies to recognize their target epitopes (Bock et al., 2011; Fuchs et al., 2011). As an example, H3K9me3 antibodies show varying degrees of sensitivity – both enhanced and perturbed epitope recognition – to neighboring PTMs that surround H3K9 (Figure S2C). Most notably, H3K9me3 antibodies we screened show differential tolerance to neighboring H3S10 phosphorylation (Figure 2B**; left**) – a mitotic combinatorial ‘methyl/phospho switch’ known to eject proteins like heterochromatin protein 1 (HP1), for example, from mitotic chromatin (Fischle et al., 2005; Hirota et al., 2005). Neighboring H3K9me3 also impacts epitope recognition by H3S10p antibodies (Figure 2B**; middle**). The H3K9me3 and H3S10p antibodies insensitive to this ‘methyl/phospho switch’ cannot distinguish between dually marked H3 tails and isolated H3K9me3 or H3S10p marks. However, several antibodies developed to recognize this methyl/phospho PTM combination are capable of this distinction by microarray analysis (Figure 2B**; right**). Collectively, these findings suggests that H3K9me3 and H3S10p antibodies sensitive to neighboring phosphorylated and methylated residues, respectively, under-represent these singly-marked histone H3 populations in mitosis, and that combinations of all three selective reagents may be required to accurately detect and map this dually marked chromatin signature.

Consistent with our previous observations (Rothbart et al., 2012e), microarray analysis shows that site-specific H4 acetyl antibodies preferentially bind epitopes with iterative increases in acetylation content (Figure 2C). For example, all of the H4K5ac antibodies screened show enhanced signal on peptides containing H4K5ac and one or more H4Kac sites, with iterative increases in acetylation content (up to 4 sites on a single peptide) being preferred epitopes for the majority of H4 acetyl antibodies screened. Importantly, this does not appear to be due to charge masking, as an H4K12ac peptide with all other lysines

mutated to glutamine (K5, K8, K16, and K20) is only recognized by H4K12ac antibodies and by a tetra-acetyl H4 antibody (4ac) that also recognizes H4K12ac peptides in isolation (Figure 2C).

## Off-target PTM recognition

A significant number of histone PTM antibodies that were screened demonstrated cross-reactivity with unintended modifications. For example, while H3K9me3 Ab2 is insensitive to neighboring H3S10p (Figure 2B**; left**) and does not recognize lower-order methylation states of H3K9 (Figure 2D), this antibody suffers from off-target recognition of other tri-methylated lysine residues, including H3K27me3, H3K23me3, and H3K18me3 (Figures 2D **and** S3). While the latter two PTMs are found in lower abundance in cells (Lin et al., 2014) and may therefore not be problematic under physiologic conditions, cross-reactivity with H3K27me3 may be problematic for this antibody, enriching for signals present in regions of facultative heterochromatin where H3K9me3 may or may not reside.

H3K9 and H3K27 are both found in an ARKS motif, and indeed, we and others have shown that the H3K9 methyltransferase G9a can modify H3K27 *in vitro* ((Tachibana et al., 2001) and not shown). While this may serve as an explanation for antibody mis-targeting between these sites, we note that this issue of off-target methyllysine reactivity does not appear to be restricted to residues found in similar sequence contexts. Indeed, analysis of H3K27me3 antibodies shows that several preferentially bind H3K4me3 peptides (Figure 3A). This off-target recognition is strongly enhanced when H3K4me3 is presented in combination with neighboring acetylation marks, a native context of H3K4me3 found in cells (Taverna et al., 2007). To test whether this cross-reactivity could be seen in cells, we performed immunoblots with this antibody on whole-cell extracts from the budding yeast *Saccharomyces cerevisiae*, an organism whose chromatin lacks H3K27 methylation (Garcia et al., 2007). To our surprise, a 17kDa band corresponding to signal from histone H3 was detected with H3K27me3 Ab3 (Figure 3B**; left**). Furthermore, this 17kDa band was undetectable following deletion of *SET1*, the sole H3K4 methyltransferase in budding yeast (Briggs et al., 2002) (Figure 3B**; right**), demonstrating cellular cross-reactivity of this H3K27me3 antibody with H3K4me3-marked histones in cells and presenting a potential conundrum for bivalency readouts (Bernstein et al., 2006) featuring these antibodies.

Another type of antibody cross-reactivity we observed was epitope recognition in the absence of a target PTM. This can be seen with several analyzed H3S10p antibodies that recognize $H3_{(1-20)}$ peptides combinatorially modified in various ways in the presence (Figure 3C**; top**) or absence (Figure 3C**; bottom**) of this phosphorylation mark. H3S10p is a dynamic histone PTM found in low abundance at transcriptionally active genes in interphase cells (Davie, 2003) and is highly enriched in mitotic chromatin during condensation (Wei et al., 1999). To confirm the behavior observed with H3S10p antibodies, we tracked the cell cycle dynamics of this PTM using an H3S10p antibody the arrays would classify as specific for this mark (Ab1) and one the arrays would classify as a pan N-terminal H3 antibody (Ab2). HeLa cell were arrested at G1/S by double thymidine block and extracts were immunoblotted at time points following release to track H3S10p through mitosis (Figure 3D). Consistent with previous observations (Davie, 2003; Wei et al., 1999), H3S10p Ab1

signal was weak through S phase and was pronounced in mitotic extracts (Figure 3D). In contrast, H3S10p Ab2 signal was equal in all cell cycle fractions, consistent with characterization by array of this antibody's behavior as an N-terminal specific, pan H3 antibody.

### ChIP validation of antibody behavior

A gold standard for histone PTM antibodies is their utility in chromatin immunoprecipitation (ChIP) assays. We therefore questioned whether characterization of antibodies by peptide microarray could inform on target recognition in ChIP. We chose two H3K27me3 antibodies that displayed acceptable behavior by peptide microarray to test in ChIP-Seq. Analysis of wild-type mouse embryonic stem cells showed a strong correlation of read distribution between the two antibodies (Figures 4A, 4B, **and** S4A). To assess the specificity of these antibodies for H3K27 methylation, parallel ChIP-Seq experiments were performed in ES cells lacking H3K27 methylation due to genetic deletion of the EED core subunit of the PRC2 histone methyltransferase complex (Chamberlain et al., 2008) (Figures 4A, 4B, S4B, and S4C). Meta-analysis of the average signal for each antibody over all H3K27 peaks in the genome (n = ~ 8,500) shows that these antibodies are specific and that signal is lost in the knockout line (Figure 4B).

While ChIP experiments comparing wild type and histone methyltransferase-null cell lines inform on antibody specificity, they can only provide correlative information on epitope recognition. We therefore sought to define more directly the specificity of histone PTM antibodies for endogenous nucleosomal epitopes by performing IPs of mouse ES cells (E14) spiked with a library of semi-synthetic DNA-barcoded mononucleosomes (Internal Standard Calibrated ChIP; IceChIP) uniformly modified by H3K4me3, H3K9me3, H3K27me3, H3K36me3, and H3K79me2 (Grzybowski et al., 2015). We tested two H3K27me3 antibodies and two H3K79me2 antibodies using both native and cross-linking IP conditions (Figures 4C and 4D). The series of semi-synthetic nucleosomes marked with H3K27me3 were significantly enriched with both H3K27me3 antibodies under both native IP and cross-linking conditions. In contrast, H3K79me2 Ab1, but not Ab2, modestly enriched for semi-synthetic nucleosomes marked with this PTM under native conditions, and neither antibody enriched for H3K79me2 nucleosomes under cross-linking conditions. Collectively, these data highlight the utility of semi-synthetic nucleosomes for histone PTM antibody characterization within ChIP experiments and suggest that the choice to cross-link chromatin in a ChIP can have consequences on the resultant IP.

## DISCUSSION

Antibody choice is the single most important element of many epigenetic experiments; yet there are many widely used commercial preparations available for a given mark, and they do not all perform equivalently. In this report, we unveil a database that documents the behavior of over 100 histone PTM-specific antibodies on peptide microarrays. This portal provides an interactive search tool, allowing investigators to access and compare antibodies based on histone type, PTM type, vendor source and other criteria. Importantly, the database is built to evolve and grow over time as additional antibodies are characterized. To facilitate

community involvement, inclusion of new antibody data can be achieved through investigator-supplied or vendor-supplied microarray results using the Upload Data tab in the main page portal. A simple user guide walks investigators through the few steps required to integrate array results on the webpage. Briefly, after an array is scanned, a three-column comma separated value (CSV) file is uploaded that contains a pixel index or spot ID number, green signal intensity and red signal intensity. A sample formatted data file is available for viewing and downloading on the site. The database and web portal are built automatically via Bash script, allowing newly acquired results to be rapidly analyzed and added to the site through a curator with minimal effort. As the need for precise characterization of an antibody's target epitope grows, the use of the array platform utilized in this report, which is commercially available through multiple vendors including EpiCypher and Millipore, will make this possible. Significantly, this database will organically grow with minimal support needed, and further, can adapt to changing array platforms.

Using the information obtained from the Histone Antibody Specificity Database, we highlight several vignettes describing the type of antibody behaviors that are seen with antibodies raised against methyllysine, acetyllysine and phosphoserine on histone residues. Antibodies examined displayed a variety of results, ranging from very specific target recognition to difficulties in recognizing a precise methyl state, acetyl site location and the specific target site itself. The antibodies exhibiting these issues could have severe consequences in data interpretation, which may depend on the abundance of the on-target mark relative to the off-target PTM. Antibody misbehavior may also be application specific (e.g., immunoblotting vs. ChIP). Our array findings revealed the capacity of some of these antibodies to show the same behavior in various applications, for example western bot (Figure 3A) and ChIP (Figure 4). Thus, the results available in the database offer an important view of each antibody and what the total possibilities are.

While another available database of antibody specificity is available (Egelhofer et al., 2011), this Antibody Validation Database (AVD) specifically offers the demonstration of an antibody's ability to work or not in western or ChIP (e.g., seeing a band in extracts or sequencing reads), but does not report on the actual specificities of each antibody for all possible target possibilities. We argue that knowing the PTM 'interactome' represents the fundamental foundation that investigators need to start with when choosing an antibody for their studies. Thus, the Histone Antibody Specificity Database is meant to complement the AVD, but not replace it. To connect these two databases, we have created hyperlinks to query available AVD data for a PTM of interest. These links are accessible by mousing over the antibody name on the heat maps (Figure S1B**)**. In addition, users can also query available ENCODE data, lot information and link directly to the product page for a given antibody from the same window.

It is important to highlight that results from the Histone Antibody Specificity Database may not translate to actual results in other applications. As mentioned above, while an antibody may show ability to bind with an off-target PTM, it may not be an issue if that off-target PTM is not present in a particular cell type, or far less abundant in bulk histones (Lin et al., 2014). Therefore, careful integration of our microarray data with available mass

spectrometry-based proteomics analysis of histone PTMs will allow investigators to predict whether off-target antibody behavior may be problematic in their specific application. However, there are likely cases where off-target recognition or failure to recognize the appropriate methyl or acetyl state can skew results, as shown in Figures 2D, 3C, 3D, 4C, and 4D. Histone core modifications like H3K79 methylation exemplify this concept. Our analysis of H3K79 methyl antibodies shows specificity on peptide arrays (as might be expected given the antibodies are raised against peptide antigens), but failure in applications where the modification must be recognized in its physiologic state. Since the peptide epitope does not represent the nucleosomal context of the mark, these antibodies fail to recognize the PTM in non-denaturing conditions (they work in denaturing assays like immunoblotting). Thus, as a first pass of selecting the right reagent, array analysis provides a high-throughput measure of the scope of on/off target binding. But as the arrays are dense surfaces of peptide epitopes, and the antibody is dilute and mono-dispersed, which is an excellent surrogate for immunoblotting and for exposed epitopes, the arrays may not represent assays like ChIP in that the format is reversed (dense surface of antibody, sparse epitope), and the nucleosomes must remain largely intact and folded.

The Histone Antibody Specificity Database represents an invaluable resource and tool for the scientific community who rely on histone PTM antibodies as detection reagents in chromatin and epigenetics research. Collectively, the data from this web portal will now greatly aid in informing investigators about specificity of antibodies they have previously used, and the website will enable better decision-making for which reagent to use in future experiments among the myriad of commercially available antibodies. It is our hope that making this specificity data publicly available will facilitate more informed antibody choices, aiding in the interpretation of results obtained with these critical reagents.

## EXPERIMENTAL PROCEDURES

### Materials

Biotinylated histone peptides (Table S1) were synthesized by Fmoc chemistry, purified by reverse phase HPLC and analyzed by MALDI-TOF MS and analytical reverse phase HPLC as previously described (Rothbart et al., 2012b). A list of antibodies screened in this study can be found in Table S2.

### Histone Peptide Microarrays

Array fabrication, antibody detection and data analysis were performed as described (Rothbart et al., 2012b) with the following modifications. Each peptide listed in Table S1 was spotted in triplicate eight times per array. Triplicate spots were averaged and treated as a single value for subsequent statistical analysis. Heat maps were generated with Java TreeView (Saldanha, 2004).

### Cell Culture, Manipulation, and Protein Harvest

HeLa cells (ATCC) were cultured in MEM (Life Technologies) supplemented with 10% FBS, maintained in a 37 °C incubator with 5% CO2 and pas saged every 2-3 days. EED-null (referred to as KO) embryonic stem cells (Gift from Weipeng Mu and Della Yee) were

generated from EED fl/fl (referred to as WT) mouse ES cells transfected with a CAG-Cre-ERT2 transgene and treated with tamoxifen. Cells were cultured as previously described (Chamberlain et al., 2008). For double-thymidine block, HeLa cells were synchronized by treatment with 2 mM thymidine (Sigma) for 16 hours, followed by release for 8 hours and retreatment with 2 mM thymidine for 16 hours. HeLa cells were lysed in cold buffer containing 10 mM PIPES (pH 7.0), 300 mM sucrose, 100 mM NaCl, 3 mM $MgCl_2$, 1× EDTA-free protease inhibitor (Roche), 1× phosphatase inhibitor cocktail (Sigma), 0.1% Triton X-100 and endonuclease (Pierce) before being resolved by SDS-PAGE. Whole cell protein extracts from wild-type (BY4741) and *set1*Δ *Saccharomyces cerevisiae* were prepared using SUMEB buffer containing 10 mM MOPS (pH 6.8), 1% SDS, 8 M urea, 10 mM EDTA and 0.01% bromophenol blue. Briefly, 500 ml of buffer and the equivalent volume of glass beads were added to approximately 36 O.D. equivalent of cells. Extracts were prepared by beating the beads for 6 minutes followed by centrifugation. Cleared extracts were serially diluted 2-fold using SUMEB buffer and boiled for 10 minutes at 95°C prior to SDS-PAGE and immunoblotting with the indicated antibodies.

## ChIP

Wild-type and EED-null ES cells were harvested and fixed for 10 minutes at room temperature in 1% formaldehyde in phosphate buffered saline (PBS) and then quenched by adding glycine to 0.125 M for 5 minutes at room temperature. 50 μL Protein A and Protein G Dynal beads (Life Technologies) were prepared by incubating with 5 μg H3K27me3 (Abcam ab6002) or 5 μg H3K27me3 (Millipore 07-449) overnight. Cells were sonicated for 10 cycles of 30 seconds on 1 minutes off using a Bioruptor (Diagenode) to an average size or 200-600 bp and incubated overnight with antibody bead complexes. The beads were washed 8 times in RIPA buffer (10 mM Tris-HCl ph 8.0, 100 mM NaCl, 1 mM EDTA, 0.5 mM EGTA, 0.1% Sodium Deoxycholate, 0.5% N-lauroylsarcosine) and eluted in 100 μL of 1% SDS, 100 mM NaHCO3 for 15 minutes at 65 degrees. Following crosslink reversal samples were treated with RNAseA and Proteinase K before purification using a Clean and Concentrator ChIP kit (Zymo Research).

## Library Preparation

Libraries were prepared using standard methods for Illumina sequencing using NEB Next ChIP kits (New England Biolabs) and samples were submitted to the UNC High-Throughput Sequencing Facility for sequencing on an Illumina HiSeq2000.

## Bioinformatics Analysis

Reads were aligned to the mouse genome (mm10) with bowtie2 using the -sensitive parameter (Langmead and Salzberg, 2012) and enriched regions were identified using macs2 v2.1.0 (Zhang et al., 2008) using the broadpeak setting. Genome browser tracks were created using the HTSeq python library (Anders et al., 2015) and are available for use as a UCSC Genome Browser track hub (GEO accession #GSE66902) at http://www.ncbi.nlm.nih.gov/geo/query/acc.cgi?token=cvmbiscshnclfud&acc=GSE66902. Comparisons of WT and KO cell lines for each antibody were carried out using R (R Core Team (2014)).

### Bar-Coded Designer Nucleosomes Construction

Barcoded semi-synthetic nucleosomes were made as previously described (Grzybowski et al., 2015). Posttranslational modifications of histone H3 included: H3K4me3, H3K9me3, H3K27me3, H3K36me3, H3K79me2, and unmodified histone H3 (WT).

### ICeCHIP

Native ICeChIP was performed with chromatin isolated from mouse ESCs (E14) as previously described (Brand et al., 2008). Aforementioned chromatin was doped with semi-synthetic nucleosomes bearing symmetrical: H3K4me3, H3K9me3, H3K27me3, H3K36me3, H3K79me2 as well as non-modified H3; each mark was identifiable by a unique DNA sequence. For crosslinked ICeChIP, the same source and amount of digested and HAP purified chromatin was subjected to a 15 minute treatment with 0.1% freshly cracked formaldehyde at room temperature. Crosslinking was extinguished with 1 volume of 2× X-link ChIP buffer (66 mM Tris pH 7.5, 300 mM NaCl, 10 mM EDTA, 2% NP-40, 0.5% N-lauroylsarcosine). The concentration of chromatin was adjusted to 20 μg/mL with appropriate ChIP buffer supplemented with 50 μg/mL BSA (NEB). 16 μL of protein A magnetic beads per IP (Dynabeads®) was washed twice with IP buffer 1 (25 mM Tris pH 7.5, 5 mM $MgCl_2$, 100 mM KCl, 10% (v/v) glycerol, 0.1% (v/v) NP-40 substitute, 50 μg/mL BSA (NEB)) and subsequently incubated with 4 uL of antibody per IP (H3K27me3 AB6002 lot GR137554; H3K27me3 AM39156 lot 29014002; H3K79me2 AM39143 lot 1008001; H3K79me2 M04-835 lot DAM1527889). Bead-antibody conjugates were subjected to two washes with ChIP buffer 1. Chromatin was incubated with antibody for 10 minutes at 4°C on a rotator.

For native ICeChIP, beads were washed twice for 10 minutes at 4°C with ChIP buffer 2 (25mM Tris pH 7.5, 5 mM $MgCl_2$, 300 mM KCl, 10% (v/v) glycerol, 0.1% (v/v) NP-40 substitute, 50 μg/mL BSA (NEB)), and once for 10 minutes at 4°C wit h ChIP buffer 3 (10 mM Tris pH 7.5, 250 mM LiCl, 1mM EDTA, 0.5% Na•Deoxycholate, 0.5% (v/v) NP-40 substitute), then briefly washed with ChIP buffer 1 and TE buffer, followed by 50 μL ChIP elution buffer (50 mM Tris pH 7.5, 1 mM EDTA, 1% w/v SDS) at 65°C for 5 minutes.

For crosslinked ICeChIP, beads were washed three times for 10 minutes at 4°C with RIPA buffer (25mM HEPES pH 7.9, 250 mM LiCl, 1mM EDTA, 1% (v/v) NP-40 substitute, 0.5% (w/v) N-lauroylsarcosine), then briefly washed with TE buffer, followed by 50 μL ChIP elution buffer (50 mM Tris pH 7.5, 1 mM EDTA, 1% w/v SDS) at 65°C for 5 minutes.

Elutions were supplemented with NaCl up to 200 mM, EDTA up to 10 mM and 20 μg of proteinase K (Roche) and incubated for 2 hours at 55°C. To purify DNA, 3 volumes of SPRI beads (18% PEG8000, 1 M NaCl, 1mg/mL Sera-Mag SpeedBeads carboxylate-modified magnetic particles) were added to the elution and pipetted 10 times up and down followed by 5 minutes incubation at room temperature. Magnetic beads were collected on the side of the tube with a magnet, and two 30 second washes with 200 μL of 80% EtOH on the magnet were performed. Tubes were then taken out of magnetic rack and 50 μL of TE buffer was added to beads and mixed by pipetting up and down.

Enrichment of each histone PTM was evaluated by qPCR using TaqMan® chemistry. Enrichment was calculated using the ΔΔCt method.

$$\text{Enrichment} = 2^{\left(Ct_{\text{input}} - Ct_{IP} - log_2(df)\right)}$$

Where df is a dilution factor between IP and input. Subsequently, enrichment for each PTM was normalized to the enrichment of the on-target nucleosome (e.g., for H3K27me3 antibody, on-target would be H3K27me3 semi-synthetic nucleosome). Experiments were performed in technical triplicate. Errors were estimated using partial derivation. All ICeChIP data has been deposited under GEO accession # GSE60378.

## Supplementary Material

Refer to Web version on PubMed Central for supplementary material.

## ACKNOWLEDGEMENTS

We thank Weiping Mu for EED null ES cells and Della Yee for assistance in culturing the ES lines. This research is supported by grants from the National Institutes of Health (NIH), CA181343 (S.B.R.), GM108367 (J.R.R.), GM100616 (S.Z.J.), GM80896 (S.M.F.) and GM110058 (B.D.S.). B.M.D. acknowledges Stephen Frye for grant support from NIH (GM100919). E.K.S. acknowledges support from an Institutional Research and Academic Career Development Award (GM000678) granted by the National Institute of General Medical Sciences, division of Training, Workforce Development, and Diversity. B.D.S. also acknowledges support from the W.M. Keck Foundation and is a co-founder of Epicypher, Inc.

## REFERENCES

Anders S, Pyl PT, Huber W. HTSeq--a Python framework to work with high-throughput sequencing data. Bioinformatics. 2015; 31:166–169. [PubMed: 25260700]

Baker M. Reproducibility crisis: Blame it on the antibodies. Nature. 2015; 521:274–276. [PubMed: 25993940]

Bannister AJ, Kouzarides T. Regulation of chromatin by histone modifications. Cell research. 2011; 21:381–395. [PubMed: 21321607]

Barski A, Cuddapah S, Cui K, Roh TY, Schones DE, Wang Z, Wei G, Chepelev I, Zhao K. High-resolution profiling of histone methylations in the human genome. Cell. 2007; 129:823–837. [PubMed: 17512414]

Bernstein BE, Mikkelsen TS, Xie X, Kamal M, Huebert DJ, Cuff J, Fry B, Meissner A, Wernig M, Plath K, et al. A bivalent chromatin structure marks key developmental genes in embryonic stem cells. Cell. 2006; 125:315–326. [PubMed: 16630819]

Bock I, Dhayalan A, Kudithipudi S, Brandt O, Rathert P, Jeltsch A. Detailed specificity analysis of antibodies binding to modified histone tails with peptide arrays. Epigenetics : official journal of the DNA Methylation Society. 2011; 6:256–263.

Brand M, Rampalli S, Chaturvedi CP, Dilworth FJ. Analysis of epigenetic modifications of chromatin at specific gene loci by native chromatin immunoprecipitation of nucleosomes isolated using hydroxyapatite chromatography. Nature protocols. 2008; 3:398–409. [PubMed: 18323811]

Briggs SD, Xiao T, Sun ZW, Caldwell JA, Shabanowitz J, Hunt DF, Allis CD, Strahl BD. Gene silencing: trans-histone regulatory pathway in chromatin. Nature. 2002; 418:498. [PubMed: 12152067]

Cai L, Rothbart SB, Lu R, Xu B, Chen WY, Tripathy A, Rockowitz S, Zheng D, Patel DJ, Allis CD, et al. An H3K36 methylation-engaging Tudor motif of polycomb-like proteins mediates PRC2 complex targeting. Molecular cell. 2013; 49:571–582. [PubMed: 23273982]

Chamberlain SJ, Yee D, Magnuson T. Polycomb repressive complex 2 is dispensable for maintenance of embryonic stem cell pluripotency. Stem cells. 2008; 26:1496–1505. [PubMed: 18403752]

Davie JR. MSK1 and MSK2 mediate mitogen- and stress-induced phosphorylation of histone H3: a controversy resolved. Science's STKE : signal transduction knowledge environment. 2003; 2003:PE33.

Dawson MA, Kouzarides T. Cancer epigenetics: from mechanism to therapy. Cell. 2012; 150:12–27. [PubMed: 22770212]

Egelhofer TA, Minoda A, Klugman S, Lee K, Kolasinska-Zwierz P, Alekseyenko AA, Cheung MS, Day DS, Gadel S, Gorchakov AA, et al. An assessment of histone-modification antibody quality. Nature structural & molecular biology. 2011; 18:91–93.

Ernst J, Kheradpour P, Mikkelsen TS, Shoresh N, Ward LD, Epstein CB, Zhang X, Wang L, Issner R, Coyne M, et al. Mapping and analysis of chromatin state dynamics in nine human cell types. Nature. 2011; 473:43–49. [PubMed: 21441907]

Fischle W, Tseng BS, Dormann HL, Ueberheide BM, Garcia BA, Shabanowitz J, Hunt DF, Funabiki H, Allis CD. Regulation of HP1-chromatin binding by histone H3 methylation and phosphorylation. Nature. 2005; 438:1116–1122. [PubMed: 16222246]

Fuchs SM, Krajewski K, Baker RW, Miller VL, Strahl BD. Influence of combinatorial histone modifications on antibody and effector protein recognition. Current biology : CB. 2011; 21:53–58. [PubMed: 21167713]

Fuchs SM, Strahl BD. Antibody recognition of histone post-translational modifications: emerging issues and future prospects. Epigenomics. 2011; 3:247–249. [PubMed: 22122332]

Funato K, Major T, Lewis PW, Allis CD, Tabar V. Use of human embryonic stem cells to model pediatric gliomas with H3.3K27M histone mutation. Science. 2014; 346:1529–1533. [PubMed: 25525250]

Garcia BA, Hake SB, Diaz RL, Kauer M, Morris SA, Recht J, Shabanowitz J, Mishra N, Strahl BD, Allis CD, et al. Organismal differences in post-translational modifications in histones H3 and H4. The Journal of biological chemistry. 2007; 282:7641–7655. [PubMed: 17194708]

Gardner KE, Allis CD, Strahl BD. Operating on chromatin, a colorful language where context matters. Journal of molecular biology. 2011; 409:36–46. [PubMed: 21272588]

Gerstein MB, Lu ZJ, Van Nostrand EL, Cheng C, Arshinoff BI, Liu T, Yip KY, Robilotto R, Rechtsteiner A, Ikegami K, et al. Integrative analysis of the Caenorhabditis elegans genome by the modENCODE project. Science. 2010; 330:1775–1787. [PubMed: 21177976]

Grzybowski AT, Chen Z, Ruthenburg AJ. Calibrating ChIP-Seq with Nucleosomal Internal Standards to Measure Histone Modification Density Genome Wide. Molecular cell. 2015 doi:10.1016/j.molcel.2015.04.022.

Hattori T, Taft JM, Swist KM, Luo H, Witt H, Slattery M, Koide A, Ruthenburg AJ, Krajewski K, Strahl BD, et al. Recombinant antibodies to histone post-translational modifications. Nature methods. 2013; 10:992–995. [PubMed: 23955773]

Hirota T, Lipp JJ, Toh BH, Peters JM. Histone H3 serine 10 phosphorylation by Aurora B causes HP1 dissociation from heterochromatin. Nature. 2005; 438:1176–1180. [PubMed: 16222244]

Jakovcevski M, Akbarian S. Epigenetic mechanisms in neurological disease. Nature medicine. 2012; 18:1194–1204.

Jenuwein T, Allis CD. Translating the histone code. Science. 2001; 293:1074–1080. [PubMed: 11498575]

Kharchenko PV, Alekseyenko AA, Schwartz YB, Minoda A, Riddle NC, Ernst J, Sabo PJ, Larschan E, Gorchakov AA, Gu T, et al. Comprehensive analysis of the chromatin landscape in Drosophila melanogaster. Nature. 2011; 471:480–485. [PubMed: 21179089]

Langmead B, Salzberg SL. Fast gapped-read alignment with Bowtie 2. Nature methods. 2012; 9:357–359. [PubMed: 22388286]

Lewis PW, Muller MM, Koletsky MS, Cordero F, Lin S, Banaszynski LA, Garcia BA, Muir TW, Becher OJ, Allis CD. Inhibition of PRC2 activity by a gain-of-function H3 mutation found in pediatric glioblastoma. Science. 2013; 340:857–861. [PubMed: 23539183]

Lin S, Wein S, Gonzales-Cope M, Otte GL, Yuan ZF, Afjehi-Sadat L, Maile T, Berger SL, Rush J, Lill JR, et al. Stable-isotope-labeled histone peptide library for histone post-translational modification

and variant quantification by mass spectrometry. Molecular & cellular proteomics : MCP. 2014; 13:2450–2466. [PubMed: 25000943]

Nishikori S, Hattori T, Fuchs SM, Yasui N, Wojcik J, Koide A, Strahl BD, Koide S. Broad ranges of affinity and specificity of anti-histone antibodies revealed by a quantitative peptide immunoprecipitation assay. Journal of molecular biology. 2012; 424:391–399. [PubMed: 23041298]

Perez-Burgos L, Peters AH, Opravil S, Kauer M, Mechtler K, Jenuwein T. Generation and characterization of methyl-lysine histone antibodies. Methods in enzymology. 2004; 376:234–254. [PubMed: 14975310]

Pesavento JJ, Bullock CR, LeDuc RD, Mizzen CA, Kelleher NL. Combinatorial modification of human histone H4 quantitated by two-dimensional liquid chromatography coupled with top down mass spectrometry. The Journal of biological chemistry. 2008; 283:14927–14937. [PubMed: 18381279]

Rothbart SB, Dickson BM, Ong MS, Krajewski K, Houliston S, Kireev DB, Arrowsmith CH, Strahl BD. Multivalent histone engagement by the linked tandem Tudor and PHD domains of UHRF1 is required for the epigenetic inheritance of DNA methylation. Genes & development. 2013; 27:1288–1298. [PubMed: 23752590]

Rothbart SB, Krajewski K, Nady N, Tempel W, Xue S, Badeaux AI, Barsyte-Lovejoy D, Martinez JY, Bedford MT, Fuchs SM, et al. Association of UHRF1 with methylated H3K9 directs the maintenance of DNA methylation. Nature structural & molecular biology. 2012a; 19:1155–1160.

Rothbart SB, Krajewski K, Strahl BD, Fuchs SM. Peptide microarrays to interrogate the “histone code”. Methods in enzymology. 2012b; 512:107–135. [PubMed: 22910205]

Rothbart SB, Lin S, Britton LM, Krajewski K, Keogh MC, Garcia BA, Strahl BD. Poly-acetylated chromatin signatures are preferred epitopes for site-specific histone H4 acetyl antibodies. Scientific reports. 2012e; 2:489. [PubMed: 22761995]

Rothbart SB, Strahl BD. Interpreting the language of histone and DNA modifications. Biochimica et biophysica acta. 2014; 1839:627–643. [PubMed: 24631868]

Saldanha AJ. Java Treeview--extensible visualization of microarray data. Bioinformatics. 2004; 20:3246–3248. [PubMed: 15180930]

Sidoli S, Cheng L, Jensen ON. Proteomics in chromatin biology and epigenetics: Elucidation of post-translational modifications of histone proteins by mass spectrometry. Journal of proteomics. 2012; 75:3419–3433. [PubMed: 22234360]

Strahl BD, Allis CD. The language of covalent histone modifications. Nature. 2000; 403:41–45. [PubMed: 10638745]

Tachibana M, Sugimoto K, Fukushima T, Shinkai Y. Set domain-containing protein, G9a, is a novel lysine-preferring mammalian histone methyltransferase with hyperactivity and specific selectivity to lysines 9 and 27 of histone H3. The Journal of biological chemistry. 2001; 276:25309–25317. [PubMed: 11316813]

Taverna SD, Ueberheide BM, Liu Y, Tackett AJ, Diaz RL, Shabanowitz J, Chait BT, Hunt DF, Allis CD. Long-distance combinatorial linkage between methylation and acetylation on histone H3 N termini. Proceedings of the National Academy of Sciences of the United States of America. 2007; 104:2086–2091. [PubMed: 17284592]

Turner BM, Fellows G. Specific antibodies reveal ordered and cell-cycle-related use of histone-H4 acetylation sites in mammalian cells. European journal of biochemistry / FEBS. 1989; 179:131–139. [PubMed: 2917555]

Wei Y, Yu L, Bowen J, Gorovsky MA, Allis CD. Phosphorylation of histone H3 is required for proper chromosome condensation and segregation. Cell. 1999; 97:99–109. [PubMed: 10199406]

Young NL, DiMaggio PA, Plazas-Mayorca MD, Baliban RC, Floudas CA, Garcia BA. High throughput characterization of combinatorial histone codes. Molecular & cellular proteomics : MCP. 2009; 8:2266–2284. [PubMed: 19654425]

Young NL, Plazas-Mayorca MD, Garcia BA. Systems-wide proteomic characterization of combinatorial post-translational modification patterns. Expert review of proteomics. 2010; 7:79–92. [PubMed: 20121478]

Zhang Y, Liu T, Meyer CA, Eeckhoute J, Johnson DS, Bernstein BE, Nusbaum C, Myers RM, Brown M, Li W, et al. Model-based analysis of ChIP-Seq (MACS). Genome biology. 2008; 9:R137. [PubMed: 18798982]

## HIGHLIGHTS

- Peptide microarrays catalogue the specificity of widely-used histone antibodies
- Histone antibodies frequently show difficulties in detecting their intended targets
- A Histone Antibody Specificity Database (www.histoneantibodies.com) was created
- This resource facilitates more informed antibody choice for epigenetic applications

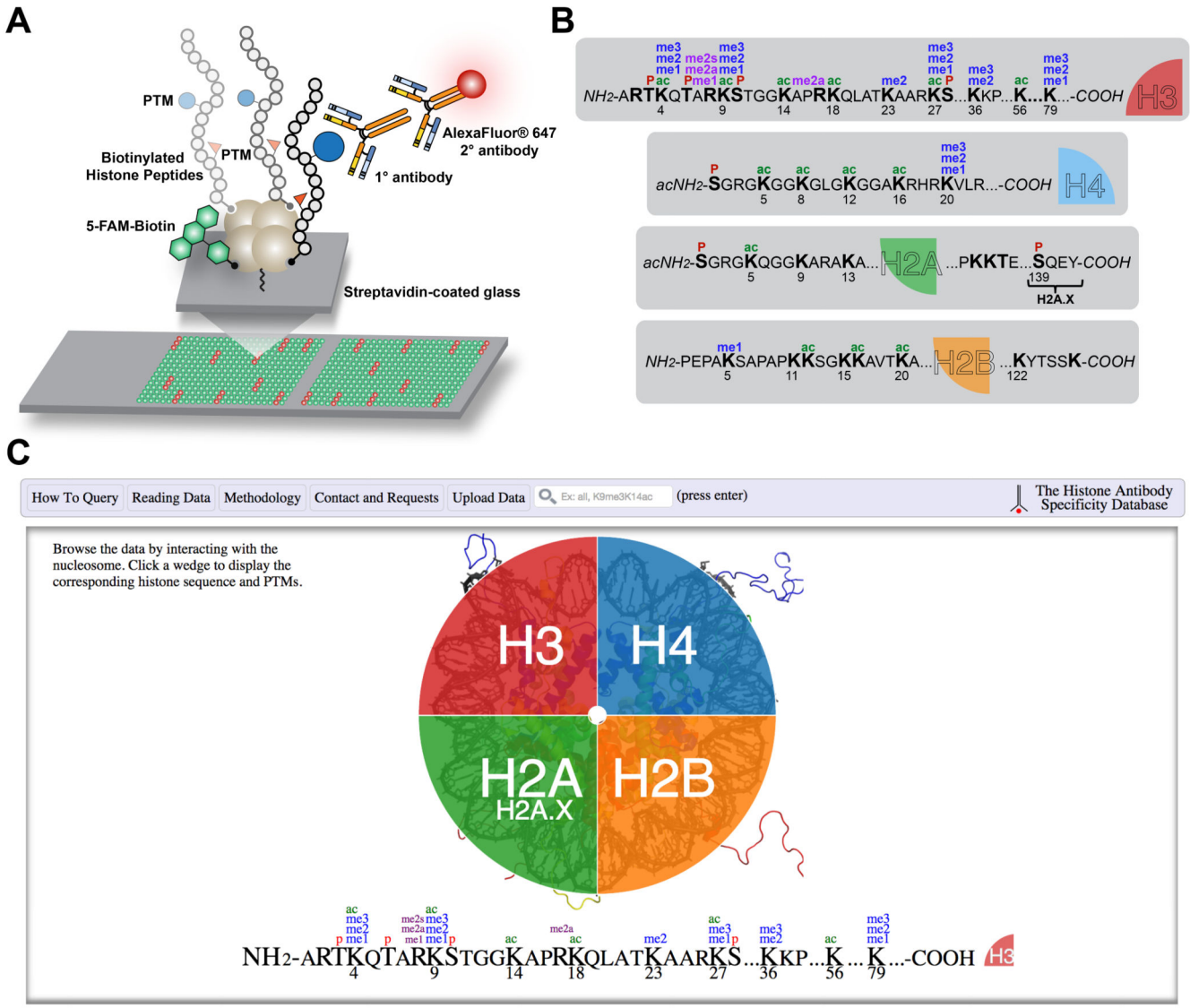


**Figure 1. Histone antibody characterization by peptide microarray and web interface of the Histone Antibody Specificity Database**

(A) Cartoon depicting the stepwise procedure for peptide microarraying of an antibody from peptide immobilization to antibody hybridization and visualization. Positive interactions are visualized as red fluorescence. All printed spots show green fluorescence from the biotinylated fluorescein (5-FAM) printing control. (B) Posttranslational modifications and their combinations on human histones for which antibodies screened to publication date (Table S2) are marketed to recognize. Lysine acetylation (ac); Lysine methylation (me1/2/3*); Arginine methylation (me1/2a/2s**); Serine and threonine phosphorylation (P). *Histone lysine methylation occurs in three forms (mono-, di-, and trimethylation). **Arginine methylation also occurs in three forms (monomethylation, symmetric, and asymmetric dimethylation). (C) Screenshot of the home page for www.histoneantibodies.com, an interactive java-based web resource displaying histone antibody specificity data from peptide microarray experiments. Users can query data by

entering strings in the search bar and by clicking on their histone and posttranslational modification of interest.

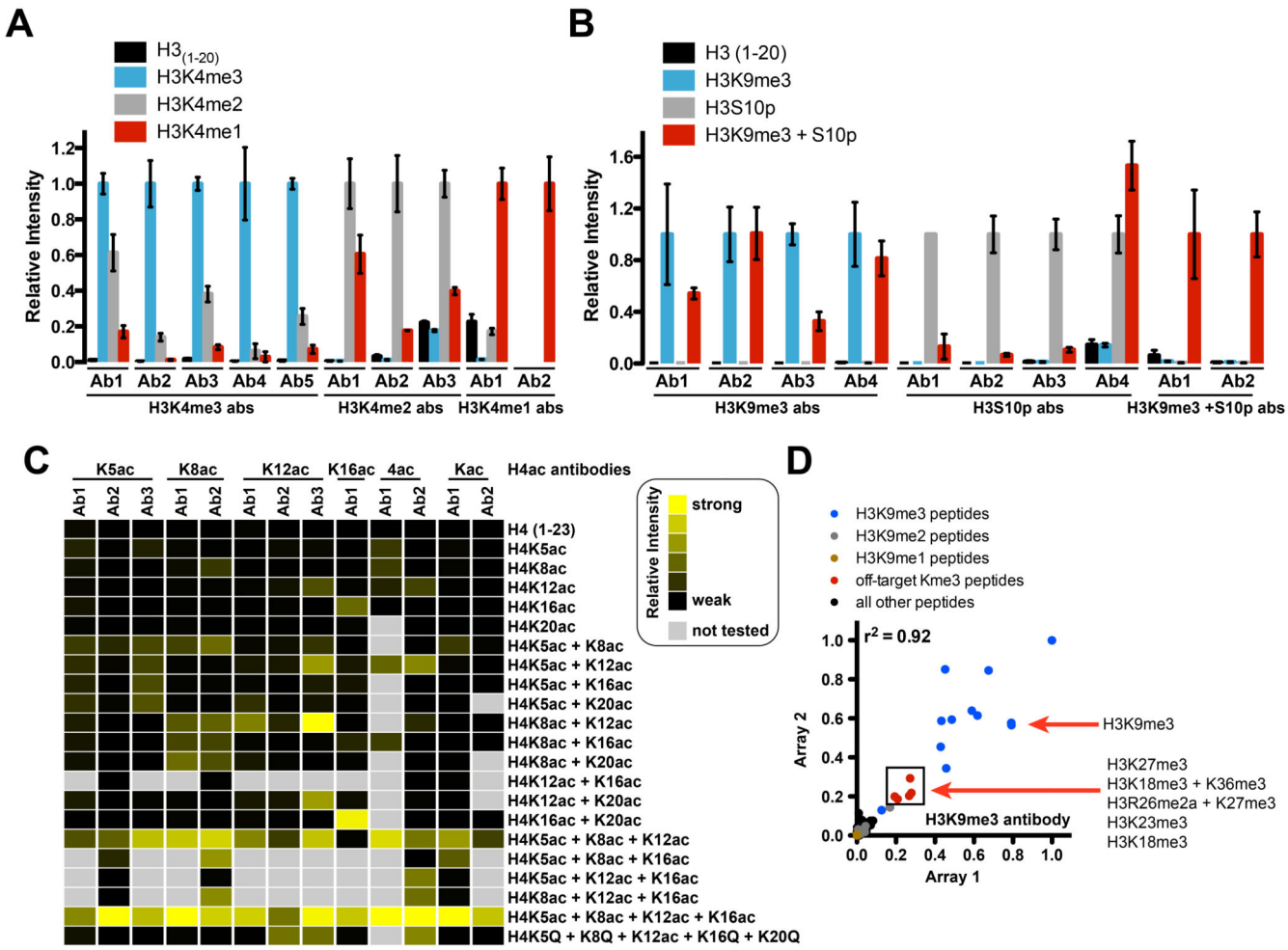


**Figure 2. Unfavorable observations of histone PTM antibody behavior**

(A) The inability to distinguish the modification state on a particular residue (e.g., mono-, di-, or trimethyl lysine). H3K4me3 and H3K4me2 antibodies cross-react with H3K4me2 and H3K4me1 peptides, respectively, to varying degrees. Average signal intensities from each antibody screened by microarray were normalized to signal from the target peptide (H3K4me3, left; H3K4me2, middle; H3K4me1, right). Error is presented as ± S.E.M. from at least two arrays. H3K4me3 Ab1 (Millipore 07-473); H3K4me3 Ab2 (Epicypher 13-0004); H3K4me3 Ab3 (Active Motif 39160); H3K4me3 Ab4 (Abcam ab8580); H3K4me3 Ab5 (Abcam ab1012); H3K4me2 Ab1 (Active Motif 39142); H3K4me2 Ab2 (Epicypher 13-0013); H3K4me2 Ab3 (Abcam ab32356); H3K4me1 Ab1 (Abcam ab8895); H3K4me1 Ab2 (Millipore 07-436). (B-C) The influence of neighboring PTMs. (B; Left) Binding of H3K9me3 antibodies to their epitopes is inhibited to varying degrees by neighboring H3S10 phosphorylation (H3S10p) and vise versa. Average signal intensities from each antibody screened by microarray were normalized to signal from the target peptide. Error is presented as ± S.E.M. from at least two arrays. H3K9me3 Ab1 (Millipore 07-442); H3K9me3 Ab2 (Diagenode C15410193); H3K9me3 Ab3 (Active Motif 39161); H3K9me3 Ab4 (Abcam ab8898); H3S10p Ab1 (Active Motif 39253); H3S10p Ab2 (Abcam ab5176); H3S10p Ab3 (Invitrogen 491041); H3S10p Ab4 (Millipore 04-817); H3K9me3 +

S10p Ab1 (Millipore 05-809); H3K9me3 + S10p Ab2 (Abcam ab5819). (C) H4 acetyl antibodies prefer poly-acetylated epitopes. Results of at least two arrays are presented as heat maps of normalized mean intensities on a scale from 0 (black; undetectable binding) to 1 (yellow; strong binding). K5ac Ab1 (Active Motif 39169); K5ac Ab2 (Active Motif 39170); K5ac Ab3 (Millipore 07-327); K8ac Ab1 (Active Motif 39172); K8ac Ab2 (Epicypher 130021); K12ac Ab1 (Active Motif 39165); K12ac Ab2 (Millipore 04-119); K12ac Ab3 (Millipore 07-595); K16ac Ab1 (Active Motif 39168); 4ac Ab1 (Active Motif 39179); 4ac Ab2 (Millipore 05-1355); Kac Ab1 (Active Motif 39925); Kac Ab2 (Millipore 06866). (D) Off-target recognition. Scatter plot showing two arrays probed with an H3K9me3 antibody (Diagenode C15410193). Analysis of H3K9 methylation states shows strong binding to H3K9me3 peptides (blue), and minimal binding to H3K9me1 (yellow) and H3K9me2 (grey) peptides. This antibody also binds off-target Kme3 peptides (red). All other peptides are shown in black. Coefficient of determination ($r^2$) was calculated by linear regression analysis using GraphPad Prism v5.

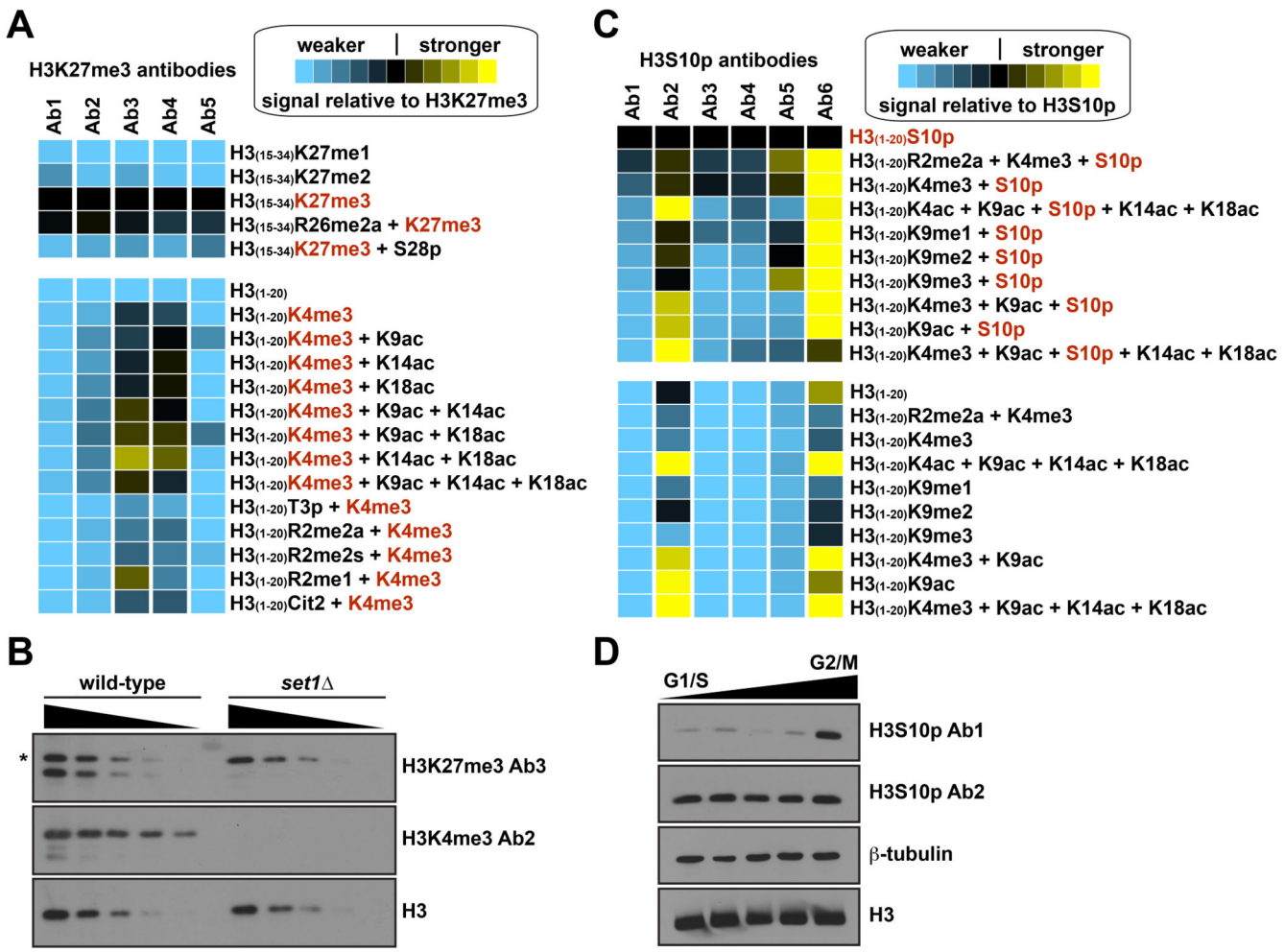


**Figure 3. Cellular validation of antibody behavior on microarrays**

(A-B) H3K27me3 antibodies bind H3K4me3 peptides. (A) Results of at least two arrays are presented as heat maps of signal intensities relative to $H3_{(15-34)}$K27me3 peptides on a scale from −1 (blue; undetectable binding) to +1 (yellow; strong binding). Ab1 (Abcam ab6002); Ab2 (Millipore 07-449); Ab3 (Active Motif 39156); Ab4 (Active Motif 39155); Ab5 (Diagenode C1541095). (B) Immunoblots of serially diluted wild-type (BY4741) and *set1*Δ yeast cell extracts. Asterisk demarcates a cross-reactive band unrelated to H3K4me3. H3K27me3 Ab2 (Active Motif 39156); H3K4me3 Ab2 (Epicypher 13-0004); H3 (Epicypher 13-0001). (C-D) H3S10p antibodies bind to the H3 N-terminal tail independent of S10 phosphorylation. (C) Results of at least two arrays are presented as heat maps of signal intensities relative to $H3_{(1-20)}$S10p peptides on a scale from −1 (blue; undetectable binding) to +1 (yellow; strong binding). Ab1 (Active Motif 39253); Ab2 (Millipore 05-598); Ab3 (Abcam ab5176); Ab4 (Invitrogen 491041); Ab5 (Millipore 04-817). (D) Immunoblots of HeLa cell extracts at 0, 2.5, 5, 7.5 and 10 hours following release from synchronization by double thymidine block. H3S10p Ab1 (Active Motif 39253); H3S10p Ab2 (Millipore 05-598).

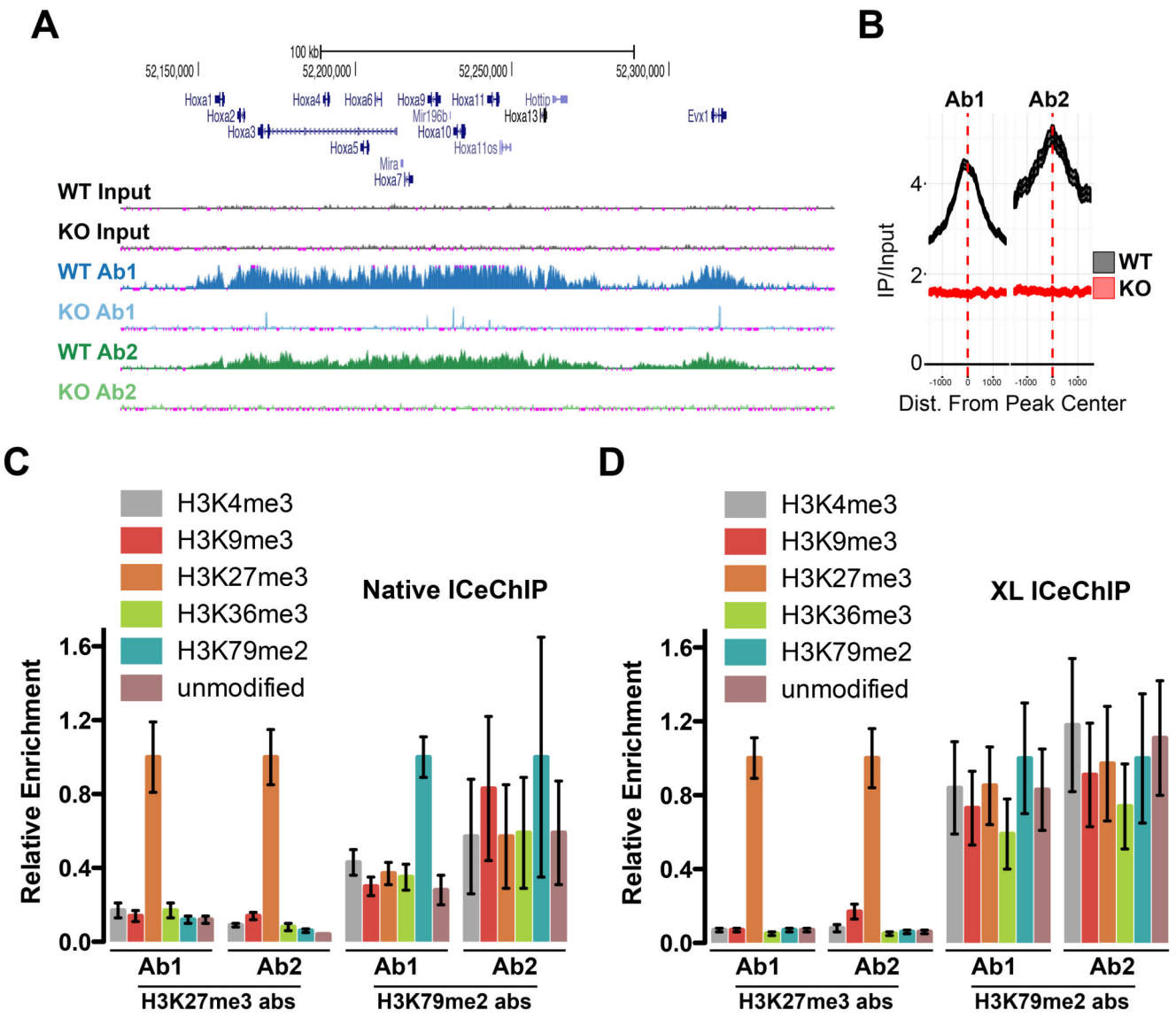


**Figure 4. Validation of antibody behavior by chromatin immunoprecipitation**

(A-B) ChIP-Seq analysis using the indicated H3K27me3 antibodies in wild-type (WT) and EED-null (KO) mouse embryonic stem cells. (A) Genome browser shot of the Hox cluster. (B) Meta-analysis of all H3K27Me3 reads 1kb on either side of transcription start sites (0) in WT (black) and KO (red) mESCs. Ab1 (Abcam ab6002); Ab2 (Millipore 07-449). (C-D) Immunoprecipitation of DNA barcoded semi-synthetic nucleosome ladders in the presence of isolated mouse native chromatin, under (C) native or (D) cross-linked conditions with the indicated antibodies. Data is presented as enrichment normalized to on-target nucleosome ± S.D. for three technical replicates. H3K27me3 Ab1 (Abcam ab6002); H3K27me3 Ab2 (Active Motif 39156); H3K79me2 Ab1 (Active Motif 39143); H3K79me2 Ab2 (Millipore 04-835).